

Impaired factor V–related anticoagulant mechanisms and deep vein thrombosis associated with A2086D and W1920R mutations

Naruto Shimonishi,^{1,2} Kenichi Ogiwara,¹ Junko Yoshida,³ Kyoji Horie,³ Yuto Nakajima,^{1,4} Shoko Furukawa,¹ Masahiro Takeyama,¹ and Keiji Nogami¹

¹Department of Pediatrics, Nara Medical University, Kashihara, Japan; ²The Course of Thrombosis and Hemostasis Molecular Pathology, Nara Medical University, Kashihara, Japan; ³Department of Physiology II, Nara Medical University, Kashihara, Japan; and ⁴Advanced Medical Science of Thrombosis and Hemostasis, Nara Medical University, Kashihara, Japan

Key Points

- FV-A2086D impaired FVa susceptibility and FV cofactor activity for APC, similar to FV-W1920R.
- FV-A2086D and FV-W1920R impaired the inhibitory effects on tissue factor–induced coagulation reactions.

Factor V (FV) plays pivotal roles in both procoagulant and anticoagulant mechanisms. Genetic mutations, FV-W1920R (FV_{Nara}) and FV-A2086D (FV_{Besançon}), in the C1 and C2 domains of FV light chain, respectively, seem to be associated with deep vein thrombosis. However, the detailed mechanism(s) through which these mutations are linked to thrombophilia remains to be fully explored. The aim of this study was to clarify thrombotic mechanism(s) in the presence of these FV abnormalities. Full-length wild-type (WT) and mutated FV were prepared using stable, human cell lines (HEK293T) and the piggyBac transposon system. Susceptibility of FVa-A2086D to activated protein C (APC) was reduced, resulting in significant inhibition of APC-catalyzed inactivation with limited cleavage at Arg³⁰⁶ and delayed cleavage at Arg⁵⁰⁶. Furthermore, APC cofactor activity of FV-A2086D in APC-catalyzed inactivation of FVIIIa through cleavage at Arg³³⁶ was impaired. Surface plasmon resonance–based assays demonstrated that FV-A2086D bound to Glu-Gly-Arg-chloromethylketone active site–blocked APC and protein S (P) with similar affinities to that of FV-WT. However, weakened interaction between FVa-A2086D and phospholipid membranes was evident through the prothrombinase assay. Moreover, addition of FVa-A2086D to plasma failed to inhibit tissue factor (TF)-induced thrombin generation and reduce prothrombin times. This inhibitory effect was independent of PC, PS, and antithrombin. The coagulant and anticoagulant characteristics of FV(a)-W1920R were similar to those of FV(a)-A2086D. FV-A2086D presented defects in the APC mechanisms associated with FVa inactivation and FV cofactor activity, similar to FV-W1920R. Moreover, both FV proteins that were mutated in the light chain impaired inhibition of TF-induced coagulation reactions. These defects were consistent with congenital thrombophilia.

Introduction

Factor V (FV) is involved in both procoagulant and anticoagulant mechanisms.^{1,2} The procoagulant activity of FV is mediated as a cofactor for activated FX (FXa) in the prothrombinase complex that

Submitted 12 September 2022; accepted 8 February 2023; prepublished online on *Blood Advances* First Edition 13 February 2023; final version published online 16 June 2023. <https://doi.org/10.1182/bloodadvances.2022008918>.

An account of this work was presented at the XXIX and XXX Congress of the International Society on Thrombosis and Haemostasis, 2021, Philadelphia, PA, and 2022, London, England, United Kingdom, respectively.

Data are available on request from the corresponding author, Kenichi Ogiwara (ogiwarak@naramed-u.ac.jp).

The full-text version of this article contains a data supplement.

© 2023 by The American Society of Hematology. Licensed under [Creative Commons Attribution-NonCommercial-NoDerivatives 4.0 International \(CC BY-NC-ND 4.0\)](https://creativecommons.org/licenses/by-nc-nd/4.0/), permitting only noncommercial, nonderivative use with attribution. All other rights reserved.

converts prothrombin to thrombin on phospholipid (PL) membranes.³⁻⁵ These reactions lead to thrombin-catalyzed proteolytic cleavages of FV at Arg⁷⁰⁹, Arg¹⁰¹⁸, and Arg¹⁵⁴⁵, resulting in its conversion to activated FV (FVa). The activated molecule is rapidly inactivated by proteolytic cleavage of the heavy chain (HCh) at Arg³⁰⁶, Arg⁵⁰⁶, and Arg⁶⁷⁹ by activated protein C (APC) and protein S (PS) to downregulate the potential for hypercoagulant reactions.^{6,7} Cleavage at Arg⁵⁰⁶ is important for the exposure of other cleavage sites but is not essential for the decrease in FVa activity^{8,9}; however, cleavage at Arg³⁰⁶ results in near complete loss of FVa activity. Nevertheless, any defect in 1 or more of these cleavage reactions influences the process of APC-induced inactivation of FVa.

Alternatively, FV functions as an anticoagulant cofactor for APC, and enhances APC/PS-catalyzed inactivation of FVIIIa through proteolytic cleavage at Arg³³⁶.^{10,11} Hence, the anticoagulant potential of FV is mediated by promoting the proteolysis by APC before thrombin cleavage. Cleavage at Arg⁵⁰⁶ of FV that still contains the B domain contributes to anticoagulant activity but cleavage at Arg³⁰⁶ is less important in this respect.^{12,13} Any molecular defect in these cleavage reactions potentiates APC resistance (APCR). The FV B domain contains an essential region that interacts with tissue factor pathway inhibitor (TFPI).^{14,15} Consequently, the anticoagulant functions of FV are associated with both APC and TFPI.^{16,17} In addition, Al Dieri et al¹⁸ identified a novel anticoagulant mechanism for FVa involving inhibition of tissue factor (TF)-induced procoagulant function, regardless of the presence of APC and TFPI. The use of recombinant human FV (rFV) may help to clarify the precise mechanism(s) of the anticoagulant properties of FV. The large size (~7.0 kb) of human FV complementary DNA, however, presents significant challenges for the stable expression of full-length FV in high yields.

APCR has been recognized as a molecular abnormality of FV involved in the pathogenesis of thrombosis. A point mutation in the FV gene, R506Q (FV_{Leiden}), is the most common defect known to affect the APC cleavage site in FV.¹ This inherited disorder impairs APC-induced inactivation of FVa directly, and via FV cofactor of FVIIIa, which has been identified in ~20% of Caucasians with deep venous thrombosis (DVT).² Other mutations, including R306T (FV_{Cambridge}),¹⁹ R306G (FV_{HongKong}),²⁰ I359T (FV_{Liverpool}),²¹ E666D,²² and A512V (FV_{Bonn})²³ have also been identified in association with DVT. These mutated residues are within the HCh, at or close to the APC cleavage site. We also previously identified a novel FV-W1920R mutation (FV_{Nara}), located in the C1 domain, remote from APC cleavage site, that is responsible for APCR-related recurrent DVT.²⁴ This mutation appeared to decrease the affinity for PL binding and for PS in the complex.²⁵ A mutation, FV-A2086D (FV_{Besançon}), in the C2 domain that is associated with APCR has recently been identified.²⁶ The individual properties of FV(a)-A2086D have previously been investigated using highly diluted plasma of the patient with the homozygous FV-A2086D as a source of the mutant FV. The study revealed that FV(a)-A2086D resulted in APCR and decreased APC-cofactor activity associated with lower affinity for PLs. In contrast, FVa-A2086D has slightly (≤ 1.5 fold) unfavorable kinetic parameters (K_m and V_{max}) of prothrombin activation compared with normal FVa. The investigators concluded that FV(a)-A2086D affects the anticoagulant pathways more strongly than prothrombinase activity. However, the detailed analyses using recombinant FV-A2086D have not been

evaluated, and the molecular relationships between these mutations and thrombophilia are yet to be fully explored.

In this study, we successfully expressed full-length rFV proteins in high yield, using a stable, human cell system with the piggyBac transposon vector. The defective mechanisms of FV-related function under the FV-A2086D mutation were investigated and FV-W1920R mutants were also studied. The data from these experiments provide novel insights into the causes of DVT in these genetic disorders.

Materials and methods

Reagents

Commercially available reagents were purchased from internationally reputable suppliers. These included restriction enzymes (New England Biolabs, Beverly, MA); infusion cloning (Takara-Bio, Otsu, Japan); specific primers (Hokkaido System, Sapporo, Japan); rFVIII (NovoEight, Novo Nordisk A/S, Bagsværd, Denmark); FV, FIXa, FX/FXa, APC, PS, and mAbAHV-5146 (Hematologic Technologies, Essex Junction, VT); α -thrombin, r-hirudin, and Glu-Gly-Arg-chloromethylketone (EGR-ck) (Calbiochem, San Diego, CA); FV-deficient, PC-deficient, PS-deficient, and antithrombin-deficient plasma (Affinity Biologicals, Ancaster, Canada); FVIII-deficient and FIX-deficient plasma (George King, Overland Park, KS); chromogenic substrate S-2222 and S-2238 (Sekisui Medical, Tokyo, Japan); rTF (Innovin; Dade, Marburg, Germany); and thrombin-specific fluorogenic substrate (Bachem, Bubendorf, Switzerland). The monoclonal antibody (mAb) C5 was kindly provided by C. Fulcher (Scripps Research, La Jolla, CA).²⁷ PL vesicles (phosphatidylserine, phosphatidylcholine, and phosphatidylethanolamine at 10%, 60%, and 30%, respectively) and EGR-APC were prepared as reported previously.^{28,29}

Vector construction

The piggyBac transposon system³⁰ was used to express wild-type (WT) and mutant FV as illustrated in supplemental Figure 1. The pPB-CAG-EBNXN sequence,³¹ which contains the constitutively active CAG promoter to express the gene of interest,³² was used as a backbone piggyBac vector. The enhanced green fluorescent protein (EGFP) coding region from pCX-EGFP³³ was amplified using the following primers: EGFP-BgSg-F1, 5'-GGCAGATC TGCATCGCCATGGTGAGCAAGGGCGAGGAGCTG-3' and EGFP-PmXh-R1, 5'-CGGCTCGAGGTTAAACTTACTTGTACA GCTCGTCCATGCC-3'. Therefore, BglII-SgfI sites and PmeI-XhoI sites were introduced upstream and downstream of the EGFP fragment, respectively. The EGFP fragment was digested with BglII and XhoI, and cloned into the BglII-XhoI site of the pPB-CAG-EBNXN, between the CAG promoter and the bovine growth hormone polyadenylation signal, yielding in pPB-CAG-EGFP-BSPX plasmid. The PGKpuroA expression cassette was excised from pPGKpuro by PstI-SalI digestion and cloned into the PstI-SalI site of the pPB-CAG-EGFP-BSPX, between the bovine growth hormone polyadenylation signal and the piggyBac transposon sequence, resulting in pPB-CAG-EGFP-BSPX-PGKpuro. The full-length WT-FV coding sequence was excised from pF1KB4969 (Kazusa DNA Research Institute, Kisarazu, Japan) by SgfI-PmeI digestion, and the EGFP region of the pPB-CAG-EGFP-BSPX-PGKpuro was replaced with this fragment using the same restriction enzymes, generating pPB-CAG-F5-PGKpuro

(supplemental Figure 1). Construction of a vector containing the mutations is described in detail in the supplemental Methods.

Expression and purification of recombinant FV

HEK293T cells were transfected with FV expression vectors and the piggyBac transposase expression vector pCMV-hyPBBase³⁴ using lipofectamine3000 (Life Technologies, Carlsbad, CA) and selected using puromycin (1 µg/mL) to stably express rFV proteins. HEK293T cells were maintained in media supplemented with 10% fetal bovine serum and ampicillin and streptomycin. After the cells became confluent, the supernatant was replaced with serum-reduced medium (Opti-MEM). FV activity (FV:C) was measured using a PT-based clotting assay. FV antigen (FV:Ag) was measured with an enzyme-linked immunosorbent assay using a Factor V-Paired Antibody set (Affinity Biologicals, Ancaster, Canada) per the manufacturer's protocol. The product was loaded onto a SP-Sepharose column and eluted with 1 M NaCl. Collected active fractions were loaded onto Q-Sepharose columns, followed by elution with 1 M NaCl. Active fractions were applied to Superd200-GL columns. Protein quantity was measured by UV analysis. The proteins were concentrated using AmiconUltra-15 (cutoff, 100 kDa).

APC-catalyzed FVa inactivation

FV (10 nM) was incubated with thrombin (10 nM) for 5 minutes at 37°C, before the addition of hirudin (5 U/mL). The FVa solution was incubated with APC (1 nM), PS (30 nM), and PL (20 µM) in HBS buffer (20 mM HEPES pH 7.2, 0.1 M NaCl, 1 mM CaCl₂, and 0.005% polysorbate20) for the indicated times.^{24,35} Aliquots were obtained from the mixtures and diluted ~30 fold. Residual FV:C was measured using PT-based clotting assays. The presence of thrombin and hirudin in the diluted samples had little effect on these assays (data not shown). FVa proteolytic cleavage was confirmed by western blotting.²⁴

FV cofactor activity for APC

FV cofactor activity for APC was measured by a FVIIIa degradation assay.³⁵ FVIII (10 nM) was activated in the presence of PL (20 µM) by thrombin (5 nM) for 30 seconds, followed by the addition of hirudin (2.5 U/mL). The generated FVIIIa was incubated with APC (2 nM) and PS (10 nM) with rFV for the indicated times in HBS buffer. Reactants were incubated with FIXa (2 nM) and FX (200 nM) for 1 minute, followed by measurement of generated FXa. Relative FVIII:C was calculated from the amounts of generated FXa. FVIIIa proteolytic cleavage was confirmed by western blotting.²⁴

Prothrombinase assay

FV (100 pM) was activated with thrombin (5 nM) for 5 minutes, followed by the addition of hirudin (2.5 U/mL). Reactants were mixed with PL and FXa, before the addition of prothrombin at the indicated concentration in HBS buffer.³⁶ Thrombin generation rates were determined after the addition of S-2238 (final concentration [*f.c.*] 0.33 mM). Thrombin generation was quantified based on a standard curve that was prepared using known amounts of thrombin.

Surface plasmon resonance (SPR)-based assay

FV interaction with EGR-APC or PS was determined using Biacore T200 (Cytiva, Sheffield, United Kingdom). EGR-APC and PS were coupled to the CM5 sensor-chip. The association of the ligand was monitored in running (HBS) buffer at a flow rate of 25 µL/min for 2 minutes. Dissociation of the bound ligand was recorded over a 2-minute period by replacing the ligand solution with buffer alone. The level of nonspecific binding, corresponding to the ligand binding to the uncoated chip, was subtracted from the signal. Rate constants for association (k_{ass}) and dissociation (k_{diss}) were determined by nonlinear regression analysis. Dissociation constants (K_d) were calculated as $k_{\text{diss}}/k_{\text{ass}}$.

Coagulation potential of FVa mutant-added plasma

1. Thrombin generation-based: FV (450 nM) samples were incubated with thrombin (5 nM) for 30 minutes, followed by the addition of hirudin (2.5 U/mL). FVa (*f.c.* 4.5 nM) was added to plasma, and thrombin generation was measured.^{18,37}
2. Diluted PT-based: PT was assessed using 100-fold diluted PT reagent (Innovin). Diluted PT reagent (50 µL) was mixed into plasma (50 µL) with FVa (4.5 nM) and incubated for 2 minutes, followed by the addition of 25 mM CaCl₂ (50 µL).

Results

Expression and purification of FV mutants

FV-WT and mutants (FV-A2086D, W1920R, and R506Q) were expressed in HEK 293T cells using the piggyBac transposon vector. FV:C and FV:Ag levels in these products are summarized in Table 1. FV:Ag in FV-A2086D and FV-W1920R mutants were reduced compared with WT but levels of FV-506Q were comparable with those of WT. These characteristics of FV mutants were consistent with those found in patient plasma samples as previously reported.^{24,26} Using sodium dodecyl sulfate–polyacrylamide

Table 1. Characteristics of FV levels (medium) and APCsr (purified preparations) in FV-WT and mutants

FV mutants	FV:C *‡	FV:Ag *§	Specific activity (fold)	APCsr †
	U/dL	µg/mL	U/µg	
FV-WT	21.3 ± 1.3	2.35 ± 0.18	0.091 (1.00)	2.12 ± 0.18
FV-A2086D (FV _{Besançon})	2.3 ± 0.1	0.29 ± 0.10	0.079 (0.86)	1.84 ± 0.16
FV-W1920R (FV _{Nara})	3.9 ± 0.1	1.04 ± 0.06	0.038 (0.42)	1.57 ± 0.14
FV-R506Q (FV _{Leiden})	20.2 ± 1.4	2.43 ± 0.22	0.083 (0.91)	1.24 ± 0.04

Measurements were performed as described in "Materials and methods." All data were measured 3 times, and the average ± standard deviation values are shown.

*Data from supernatant in media.

†Data from purified preparations.

‡FV:C, FV activity was measured by using a PT-based 1-stage clotting assay.

§FV:Ag, FV antigen level was measured by an ELISA.

||APCsr, APC sensitive ratio was measured by an aPTT-based assay as described in supplemental Methods.

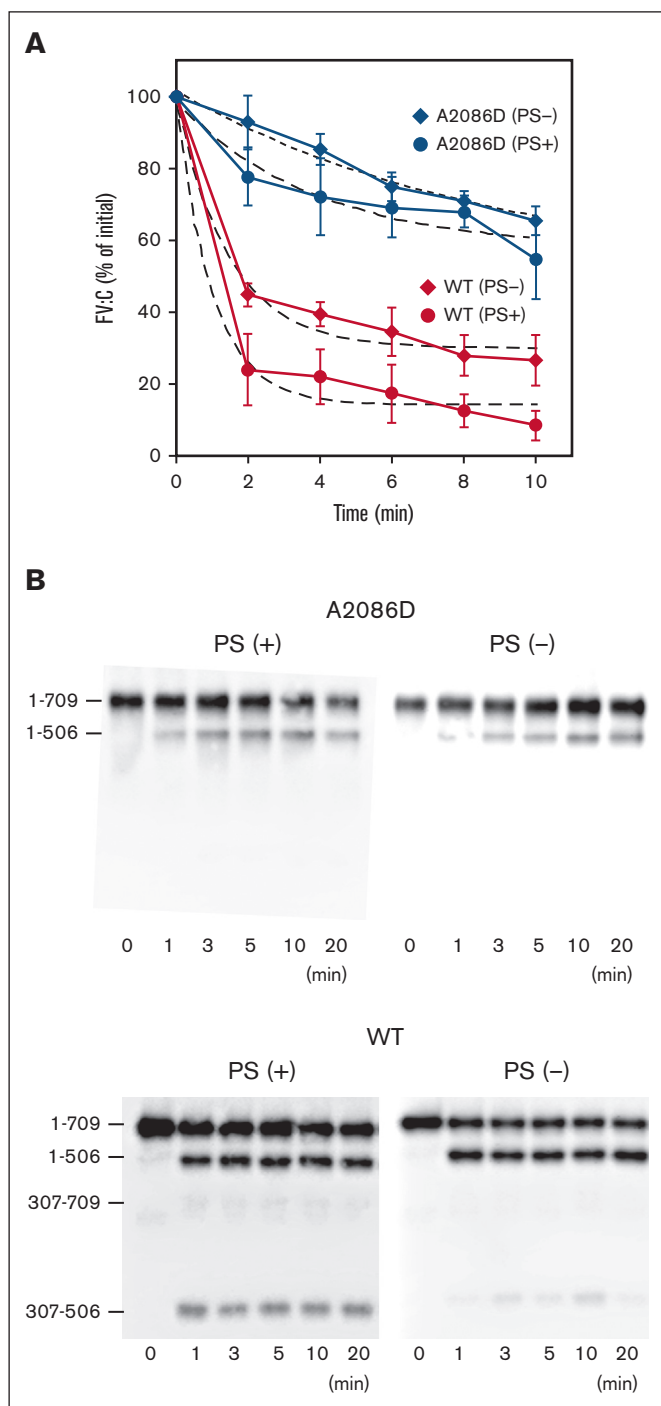


Figure 1. APC-mediated inactivation and cleavage of FVa-A2086D. (A) APC-mediated inactivation. FV-WT and FV-A2086D (10 nM) were incubated with thrombin (10 nM) for 5 minutes, followed by the addition of hirudin (5 U/mL). FVa (2 nM) was reacted with APC (1 nM) and PL (20 μ M) in the presence or absence of PS (30 nM) for the indicated times. After dilution, FVa activity (FVa:C) was measured via a PT-based clotting assay. An initial FVa:C was regarded as 100%. Experiments were performed at least 3 times, and average values \pm standard deviations are shown. The plotted data were fitted using an equation of single exponential decay (dashed lines). The rate constants (min^{-1}) obtained were FV-WT; 1.02 ± 0.26 (plus PS) and 0.68 ± 0.15 (minus PS), and FV-A2086D; 0.26 ± 0.15 (plus PS) and 0.11 ± 0.05 (minus PS). (B) APC-catalyzed proteolytic cleavage of the HCh

gel electrophoresis (SDS-PAGE), the purity of the rFV proteins was confirmed to be $>90\%$ (supplemental Figure 1B). APCR was confirmed using an aPTT-based APCR assay, for which all mutations are shown in Table 1.

APC-catalyzed inactivation and cleavage of FVa-A2086D

APC-catalyzed inactivation of the FVa mutant was examined using a PT-based clotting assay to investigate residual FVa activity (Figure 1A). In the presence of PS, FVa-WT activity (FVa-WT:C) rapidly decreased after the addition of APC, and had declined to between $\sim 20\%$ and 30% of its initial level at 2 minutes. However, FVa-A2086D:C decreased more slowly and remained at $\sim 60\%$ of initial activity at 10 minutes. The inactivation rate constant of FVa-A2086D was ~ 4 -fold lower compared with that of FVa-WT. In the absence of PS, FVa-WT:C was inactivated after the addition of APC and had declined to $\sim 30\%$ of the initial level at 10 minutes, whereas FVa-A2086D:C remained at $\sim 70\%$ of the initial level. The inactivation rate of FVa-A2086D was ~ 6 fold lower than that of FVa-WT.

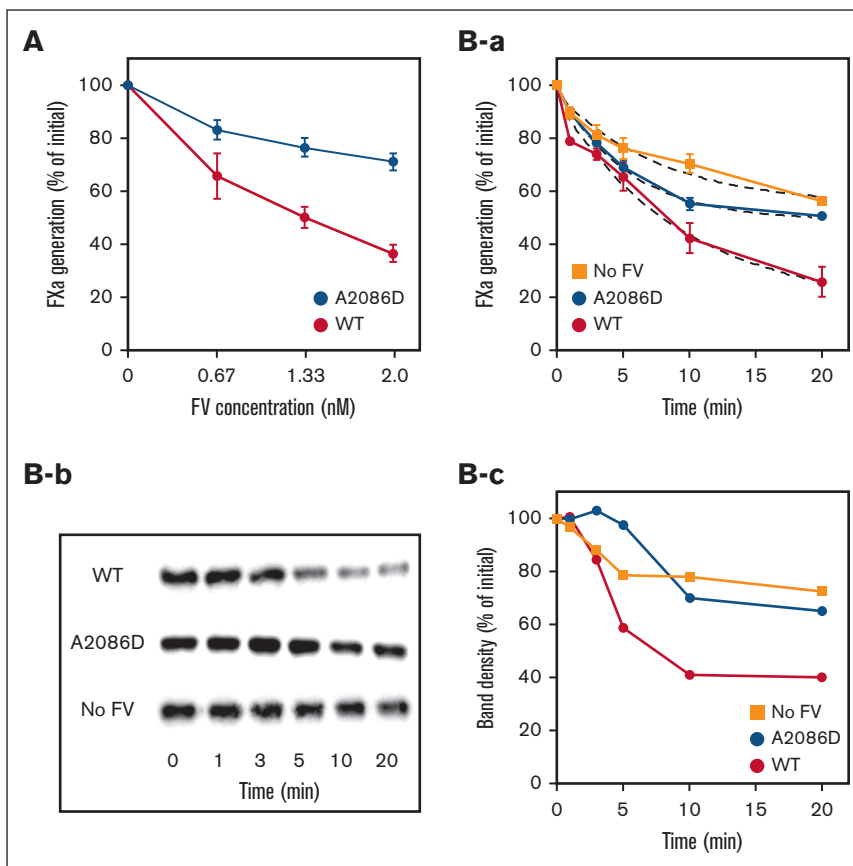
SDS-PAGE analyses of APC cleavage were designed to investigate the mechanism(s) contributing to disordered APC-catalyzed FVa inactivation (Figure 1B). In the presence of PS, the 1-506 fragment band rapidly appeared in FVa-WT within 1 minute after the reaction with APC, followed by 307-506 bands, demonstrating rapid and consecutive cleavage at Arg⁵⁰⁶ and Arg³⁰⁶. In the absence of PS, cleavage at Arg³⁰⁶ was not readily apparent after a 20-minute incubation, confirming the contribution of PS in cleavage at Arg³⁰⁶ (lower panels). The appearance of the 1-506 band in FVa-A2086D was markedly delayed relative to its appearance in WT, and cleavage at Arg³⁰⁶ was not detected, regardless of the presence of PS (upper panels). These results suggest that the impaired APC-catalyzed inactivation of FVa-A2086D was owing to markedly delayed cleavage at Arg⁵⁰⁶ and limited cleavage at Arg³⁰⁶, independently of PS. These data also indicate that these mutations might directly interfere with APC and/or PS interactions, similar to that of FVa-W1920R.^{24,25}

FV-A2086D as a cofactor in APC-catalyzed inactivation of FVIIIa

The characteristics of FV-A2086D as a cofactor of APC were examined using a FVIIIa degradation assay (Figure 2). FV-WT enhanced APC-catalyzed inactivation of FVIIIa in a dose-dependent manner. FXa generation was decreased by $\sim 60\%$ at the maximum concentration of FV-WT used (2 nM) compared with the control in the absence of FV. FV-A2086D also moderated FXa generation but the effects were less than those observed with FV-WT ($\sim 30\%$ of control). The time courses of APC-catalyzed inactivation of FVIIIa are illustrated in Figure 2Ba. FXa generation was decreased to between $\sim 20\%$ and 30% of that in the control after

Figure 1 (continued) of FVa-A2086D. FV-WT and FV-A2086D (5 nM) were incubated with thrombin (5 nM) for 5 minutes, followed by the addition of hirudin (2.5 U/mL). Generated FVa was incubated with APC (1 nM) and PL (20 μ M) in the presence or absence of PS (30 nM) for the indicated times. Samples were analyzed on 8% gels, followed by western blotting using an anti-FV HCh mAb 5146 immunoglobulin G.

Figure 2. APC cofactor activity of FV-A2086D on APC-induced FVIIIa degradation. (A) FVIIIa inactivation. FVIII (6 nM) with PL (20 μ M) was activated by thrombin (5 nM), followed by the addition of hirudin (2.5 U/mL). Generated FVIIIa was incubated either with mixtures of APC (1 nM), PS (10 nM), and FV-WT or FV-A2086D (0-2 nM) for 20 minutes. FXa generation was initiated by the addition of FIXa (2 nM) and FX (200 nM) for 1 minute. Values of FXa generation in the absence of FV were regarded as 100%. All experiments were performed at least 3 times, and the average values are shown. (B) FVIIIa inactivation and A1 cleavage at Arg³³⁶ in FVIIIa by APC. rFVIII (6 nM) with PL (20 μ M) was activated by thrombin (5 nM) for 30 seconds, followed by the addition of hirudin (2.5 U/mL). Generated FVIIIa was incubated with mixtures of APC (2 nM), PS (10 nM), with or without FV-WT or FV-A2086D (2 nM) for the indicated times. (Ba) FXa generation was initiated by the addition of FIXa (2 nM) and FX (200 nM) for 1 minute. The data were fitted using an equation of single exponential decay (dashed lines). All experiments were performed at least 3 times, and the average values are shown. The rate constants (min^{-1}) obtained were FV-WT, 0.19 ± 0.02 ; FV-A2086D, 0.13 ± 0.05 ; no FV, 0.11 ± 0.04 . (Bb) The same samples as in panel B were analyzed on 8% gels, followed by western blotting using an anti-A1 mAbC5 immunoglobulin G. (Bc) Band densities of intact A1¹⁻³⁷² observed from panel b were measured by quantitative densitometry. The density before the addition of APC was regarded as 100%.



20 minutes in the presence of FV-WT. However, in the presence of FV-A2086D, FXa generation was restricted to only ~50% of that of the control at the same time point. The rate of FVIIIa degradation in FV-A2086D was ~0.68 fold of that of WT, and the degree of this rate was almost comparable with that observed in the absence of FV.

APC-catalyzed inactivation of FVIIIa is regulated by cleavage at Arg³³⁶ in the A1 domain of FVIII.³⁸ Figure 2Bb,c illustrates the time-dependent cleavage at Arg³³⁶ and the changes in band density analyzed by western blotting using mAb C5, which recognizes residues 351-365 epitope. In using this technique, the disappearance of the A1 band identifies cleavage at Arg³³⁶.³⁹ For FV-WT, the band density of intact A1 decreased gradually in a time-dependent manner. In contrast, the disappearance of the A1 band in FV-A2086D was markedly delayed, similar to the condition without FV. These results suggest that the APC cofactor activity of FV-A2086D was significantly impaired.

Impact of PL on prothrombinase activity with FVa-A2086D

The interactions of FV-A2086D with PL were further examined using a prothrombinase assay. The results are shown in Figure 3 and summarized in Table 2. With FVa-A2086D, the K_d value for PL vesicles was ~22 fold greater than with FVa-WT, showing that FVa-A2086D had reduced affinity for PL. In addition, the K_d value for Fxa was ~2-fold greater with FVa-A2086D than with FVa-WT. However, similar K_m values for prothrombin were recorded between FVa-A2086D and FVa-WT, as previously reported.²⁶

Direct binding of FVa-A2086D to immobilized EGR-APC or PS

Our findings were consistent with defective APC-related mechanisms associated with FV-A2086D,²⁶ similar to FV-W1920R.²⁴ To examine the influence of FV mutant interaction with APC or PS, direct binding for these interactions was investigated using semifluid-phase SPR-based assays. Active site-blocked EGR-APC was used in these experiments to limit APC proteolysis of the FV molecule. For this experiment, in addition to FV-A2086D, 2 FV mutants with APCR, FV-W1920R and FV-R506Q, were prepared. Figure 4A-B shows binding curves corresponding to the association and dissociation of FV mutants on immobilized EGR-APC or PS, respectively. The data were analyzed by nonlinear regression using a 1:1 binding model with a drifting baseline. Based on the blood concentrations of FV, PC, and PS, the differences in the K_d values between FV-A2086D, FV-W1920R, FV-R506Q, and FV-WT for binding to either EGR-APC or PS seemed unlikely to be significant (Table 3). These findings suggest limited disturbance in the binding of FV-A2086D and FV-W1920R to EGR-APC and PS. However, interpretation of these data is limited, because of the absence of PL, and its interaction with FV instead of FVa.

Inhibitory effect of FVa mutants on TF-induced procoagulant function

Additional mechanism(s) related to DVT other than APCR were examined by focusing on possible inhibitory reactions of the LCH region in FVa, using TF-induced thrombin generation assays.¹⁸

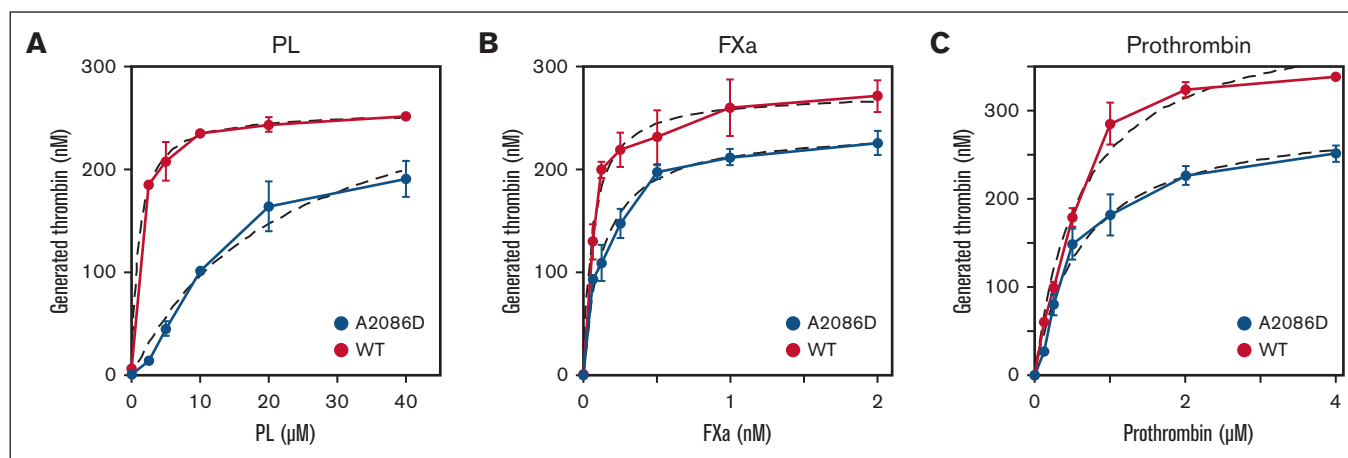


Figure 3. Impact of PL, FXa, and prothrombin on prothrombinase activity reacted with FVa-A2086D. FV-WT and FV-A2086D (100 pM) was activated by thrombin (5 nM) for 1 minute, before the addition of hirudin (2.5 U/mL). FVa was mixed, (A) with FXa (1 nM) and prothrombin (1 μM) and various concentrations of PL (0-40 μM), (B) with various concentrations of FXa (0-2 nM) and prothrombin (1 μM) and PL (10 μM), or (C) with FXa (1 nM) and various concentrations of prothrombin (0-4 μM) and PL (10 μM). The reactions were quenched with EDTA (*f.c.* 50 mM). Rates of thrombin generation were determined after the addition of S-2238. Thrombin generation was quantified by extrapolation from a standard curve prepared using known amounts of thrombin. The plotted data were fitted using the Michaelis-Menten equation (dashed line) and the K_m and V_{max} values for FVa-dependent FXa-catalyzed prothrombin activation were calculated. Experiments were performed at least 3 times, and the average values \pm standard deviations are shown.

Therefore, we speculated that FVa-A2086D and FV-W1920R mutated in the LCh may exacerbate the inhibitory effect on thrombin generation, and FV-R506Q mutated in the HCh may exhibit an inhibitory effect similar to that of FV-WT. FVa mutants were added to pooled normal plasma before evaluating TF-induced thrombin generation. Exogenous FVa-A2086D and FVa-W1920R mutants had little effect on thrombin generation, whereas the addition of FVa-WT and FVa-R506Q mutant severely decreased peak levels of thrombin activity (Figure 5A). Thrombin generation patterns like those with FVa-A2086D and FVa-W1920R were demonstrated in control experiments in the absence of FVa. We confirmed that small amounts of thrombin and hirudin had no effect on thrombin generation (data not shown). Similar results were obtained with AT-, PC-, and PS-deficient plasmas (Figure 5B-D), suggesting that the inhibitory effects were independent of these factors.

Alternative experiments were also conducted by adding FVa mutants to pooled normal plasma, followed by measuring prothrombin times (PTs) with a diluted PT reagent (Figure 6). Exogenous FVa-WT and FVa-R506Q prolonged the PT, consistent with the inhibition of procoagulant function. However, PT in the presence of FVa-A2086D and FVa-W1920R were comparable to

plasma without FVa. Small amounts of thrombin and hirudin had no effect on diluted PT assays (data not shown). These results demonstrate that FVa-A2086D and FVa-W1920R mutants had lost the ability to moderate TF-induced procoagulant activity. In addition, we confirmed that similar results were obtained using AT-, PC-, and PS-deficient plasmas (Figure 6B-D, respectively), consistent with the results obtained for thrombin generation.

Discussion

We have successfully expressed full-length FV in HEK293T cells using the piggyBac transposon system.^{30,31} To the best of our knowledge, there have been no reports of a stable, human cell line expressing full-length FV. The piggyBac transposon, originally isolated from the cabbage looper moth *Trichoplusia ni*, is highly active in mammalian cells,³¹ and mobilizes 100-kb DNA fragments.⁴⁰ Moreover, the technique was successfully used for the *in vivo* delivery of FVIII.⁴¹ Supplementary histone deacetylase inhibitors are shown to increase expression of recombinant FV in baby hamster kidney cells,⁴² but our method enabled higher levels of expression using human cells without modification of the culture medium. The results suggest that the piggyBac transposon offered a promising approach for the expression of other factors.

Castoldi et al,²⁶ using patient plasma, reported that FV-A2086D exhibited APCR. However, sufficient amounts of recombinant FV could not be obtained, and, as the authors described, an influence of plasma components could be not fully excluded. In this study, we again confirmed that recombinant FV-A2086D exhibited APCR. Compared with FV-WT, the binding affinity of FVa-A2086D with FXa and prothrombin were not significantly different from what was previously reported.²⁶ Similar to that reported by Castoldi et al,²⁶ the effect of PS was reduced in APC-induced inactivation, compared with WT, similar to that observed with FV-W1920R. In addition, we confirmed that FV cofactor activity in FVIIIa inactivation was reduced, similar to FV-W1920R.

Table 2. Kinetic parameters of the prothrombinase activity of FV mutants

FV mutant	K_d		K_m
	PL μM	FXa nM	Prothrombin μM
FV-WT	1.02 \pm 0.21	0.061 \pm 0.016	0.675 \pm 0.126
FV-A2086D	22.2 \pm 2.8	0.129 \pm 0.013	0.708 \pm 0.066

Reactions performed are described in "Materials and methods." Kinetic parameters were calculated by fitting the data presented in Figure 3. Data are shown as average \pm standard deviation values.

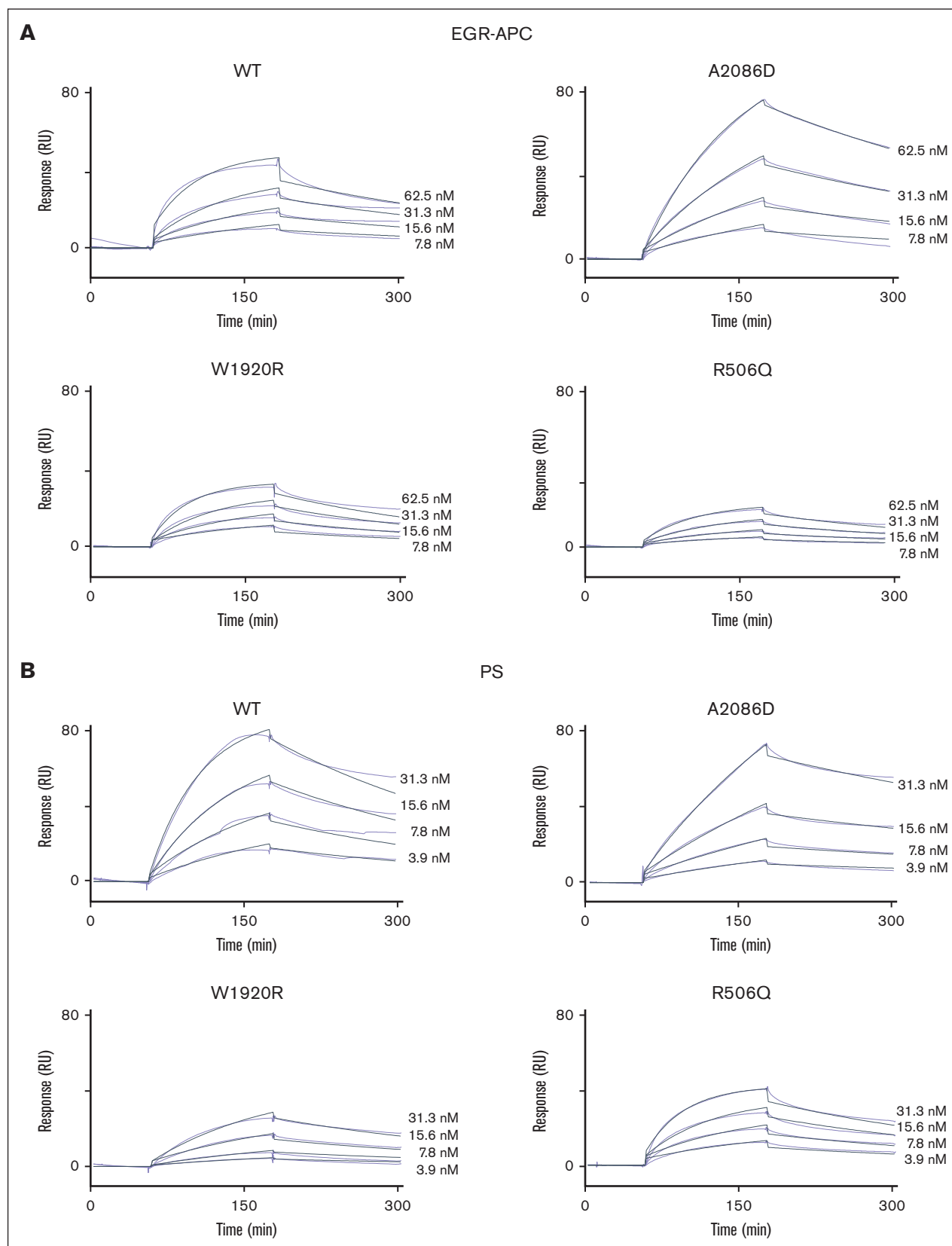


Figure 4. Direct binding of the FV mutants to EGR-APC and PS by a fluid-phase SPR-based assay. (A) EGR-APC binding. Various concentrations of FV mutants (WT, A2086D, W1920R, and R506Q) were added to EGR-APC (700 RU) immobilized on the sensor chip for 4 minutes, followed by a change of running buffer for 4 minutes. The lines

Table 3. Binding parameters of the interaction of FV mutants and immobilized EGR-APC or PS in an SPR-based assay (BIAcore)

FV mutant	EGR-APC immobilized				PS immobilized			χ^2
	k_{ass} $\times 10^5 \text{ M}^{-1} \text{ s}^{-1}$	k_{diss} $\times 10^{-3} \text{ s}^{-1}$	K_{d} nM	Chi2	k_{ass} $\times 10^5 \text{ M}^{-1} \text{ s}^{-1}$	k_{diss} $\times 10^{-3} \text{ s}^{-1}$	K_{d} nM	
WT	3.37	3.59	10.7	1.29	5.20	3.93	7.56	1.76
A2086D	1.32	2.68	20.3	0.824	9.84	1.93	19.6	0.919
W1920R	3.38	4.33	12.8	0.832	1.45	3.82	26.2	0.708
R506Q	2.39	4.57	19.1	0.106	7.11	3.74	5.26	0.960

Reactions were performed as described in "Materials and methods." Parameter values were calculated by nonlinear regression analysis from data in Figure 4A-B using the evaluation software provided by Biacore AB.

EGR-APC, EGR active site-blocked APC.

Pioneering studies established that FV(a) bound to APC on the PL membrane,⁴³ and later reports demonstrated that FVa residues 311-325 represent an APC-binding region.⁴⁴ The current data using an SPR-based assay confirmed that variant FV bound directly to APC in the absence of PL. However, in this study's APC-related investigations, no significant differences between FV-A2086D, FV-W1920R, and FV-WT were observed. Therefore, results from this study suggested that mutations in the C1 and C2 domains are unlikely to affect APC associations. However, we performed an SPR-based assay using FV instead of FVa, in the absence of PL, and therefore, interpretation of APC-induced FVa inactivation from these data might be limited. The results support, however, that the reduction in cofactor function for FVIIIa inactivation would be because of other factors and not the reduced affinity of APC.

Gierula et al²⁵ concluded that membrane interactions between FVa-W1920R and PS are essential for FVa cofactor function. Our SDS-PAGE analyses clearly demonstrated that FV-A2086D and FV-W1920R²⁴ were not proteolyzed by APC at Arg³⁰⁶, irrespective of the presence of PS, and our assays of FVa activity indicated that these mutations interfered with APC function. Minimal differences were observed, however, in direct interaction of PS with FV-A2086D and FV-W1920R, compared with FV-WT. Structural analysis of FV/FVa by cryoelectron microscopy revealed that the 2 C domains in FV are similar to each other,⁴⁵ however, some differences are evident in FVa. The C2 domain exhibits an open conformation that penetrates the PL bilayer, and in silico analysis revealed that FV-A2086D and FV-W1920R might display a more closed conformation.²⁶ Both mutations seem to affect near-homologous residues in the C1 or C2 domain, causing comparable structural changes and modifying PL-binding properties. We thought that the APCR of FV-A2086D and FV-W1920R was caused by defective interactions of FVa with APC or PS, or association with PL in the FV(a)/PS/APC complex, which is also based on previous reports.^{25,26}

FVa markedly inhibits TF-induced thrombin generation,¹⁸ a function considered to be related to the LCh fragment of FV. This study indicated that inhibitory mechanisms were severely impaired in FV-A2086D and FV-W1920R, mutated in the C1 and C2 domain,

respectively. FV-R506Q, with a mutation in the A2 domain demonstrated an anticoagulant effect similar to FV-WT. Furthermore, clotting times using a diluted PT assay showed similar results. Our findings support the argument of Al Dieri et al,¹⁸ and strongly suggest that these defective molecular interactions could contribute to thrombosis in patients with FV-A2086D and FV-W1920R. Confirmatory data were also obtained using TFPI-, FIX-, and FVIII-deficient plasma samples in the diluted PT assays (supplemental Figure 2). These results indicate that the inhibitory effect of FVa is independent on these factors, as suggested by Al Dieri et al.¹⁸

In a clinical context, this report could help improve the assessment and risk of thrombophilia. The reported mean age at the first thrombotic event in patients homozygous for the FV R506Q mutation was 25 years (range, 10-40 years) and 36 years (ranges 18-71) for heterozygotes.⁴⁶ However, only a single case of FV-A2086D and FV-W1920R was reported,^{24,26} and it is difficult to compare age-related risks in these instances, although both patients developed thromboses as teenagers. Our assays of aPTT-based APCr, which are usually used to evaluate APCr, showed progressively less APCr in the order of FV-R506Q, FV-W1920R, and FV-A2086D. However, the inhibitory effect of LCh of FV was not observed with the aPTT reagent (data not shown), consistent with q previous report that the intrinsic pathway was not involved.¹⁸ Therefore, we used the diluted PT reagent instead of the aPTT reagent for the APCr assay to evaluate anticoagulant function potential that reflect both APCr and an inhibitory effect. The clotting time of FV-deficient plasma mixed with FV-WT in the presence of APC was prolonged by 1.48 ± 0.08 fold. However, that of FV-deficient plasma mixed with FV-A2086D, FV-W1920R, and FV-R506Q was prolonged by 1.07 ± 0.02 , 1.08 ± 0.02 , and 1.10 ± 0.06 fold, respectively (supplemental Table 2), suggesting similar levels of APCr in all mutants. The diluted PT-based APC sensitivity ratio may offer a more appropriate assessment of APCr in patients with genetic FV defects.

This study has some limitations. The important relationship between FV and TFPI was identified in an inherited bleeding disorder linked to the FV variant, A2440G (FV_{East Texas}).⁴⁷ FV

Figure 4 (continued) show representative curves for FV mutants at 7.8, 15.6, 31.3, and 62.5 nM, and the fitted curves prepared using a 1-site binding model are shown (solid thin line). (B) PS binding. Various concentrations of FV mutants (WT, A2086D, W1920R, and R506Q) were added to PS (3000 RU) immobilized on the sensor chip for 2 minutes, followed by a change of running buffer for 2 minutes. The lines show representative curves for FV mutants at 3.9, 7.8, 15.6, and 31.3 nM, and fitted curves prepared using a 1-site binding model are shown (solid thin line).

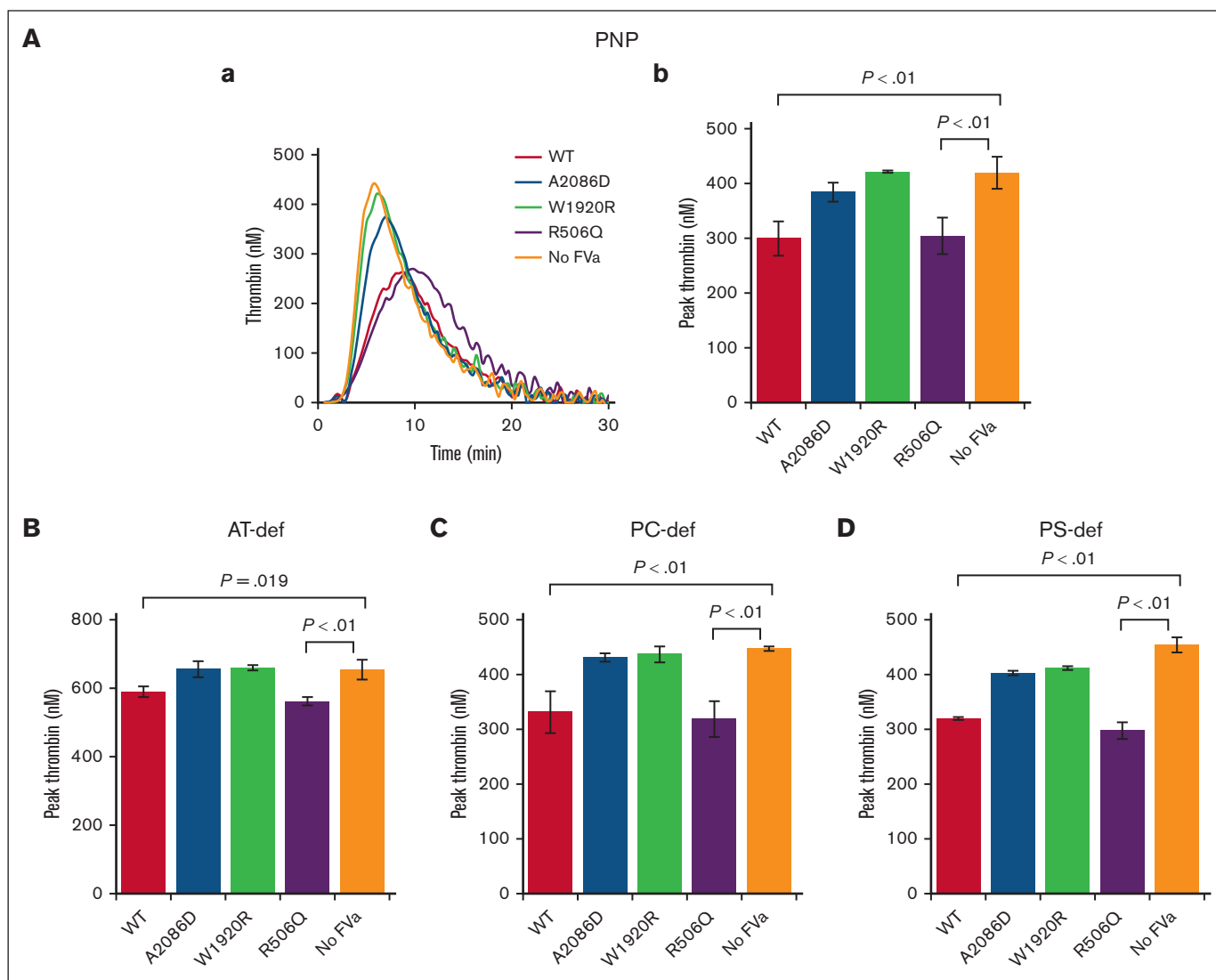


Figure 5. Inhibitory effects on TF-triggered thrombin generation of the addition of FVa mutants to anticoagulant-deficient plasmas. FV mutants (WT, A2086D, W1920R, and R506Q) and no FV were incubated with thrombin (5 nM) for 30 minutes, and reactions terminated by the addition of hirudin (2.5 U/mL). The generated FVa (*i.e.* 4.5 nM) was added to plasma, followed by the measurement of thrombin generation after the addition of TF (5 μ M) and PL (4 μ M). (A) Representative thrombin-generation curves (Aa) and peak thrombin parameter (Ab) on the addition of FVa in pooled normal plasma are shown. Peak thrombin after the addition of FVa to (B) antithrombin (AT)-deficient, (C) PC-deficient, and (D) PS-deficient plasma are shown. Experiments were performed at least 3 times, and the average values \pm standard deviations are shown. One-way analysis of variance was performed on experimental data.

appeared to enhance the function of TFPI, along with PS, during the initial coagulation phase.⁴⁸ FV possesses anticoagulant activity in plasma in the presence of TFPI.⁴⁹ Because the relationship between FV and TFPI was not investigated in the present study, this is a topic for future work. We have successfully evaluated the association of FV with APC and PS but, as mentioned earlier, we need to evaluate the association of FVa with APC and PS, and it would be important to evaluate the binding affinity on the PL membranes. Furthermore, regarding the inhibitory effect of LCh of FV, we used FVa and could not perform the same experiment using the isolated LCh of FV. Further investigation is required to clarify the precise mechanism(s).

We conclude that FV-A2086D presented defects in APC mechanisms associated with FVa susceptibility and FV cofactor activity for APC. In addition, anticoagulant function of FV was attributed to an inhibitory effect on TF-induced procoagulant activity, and was defective in FV-A2086D and FV-W1920R, mutated within the LCh. The impaired FV/FVa-associated anticoagulant properties of FV-A2086D included the diminished FVa susceptibility and defective FV cofactor activity of APC, inhibition of TF-induced procoagulant function, and low levels of TFPI.²⁶ Furthermore, FVa, FV cofactor, and TF-related abnormalities were evident in FV-W1920R. These disordered reactions appeared to represent a hypercoagulable phenotype, likely enhancing the risk of DVT.

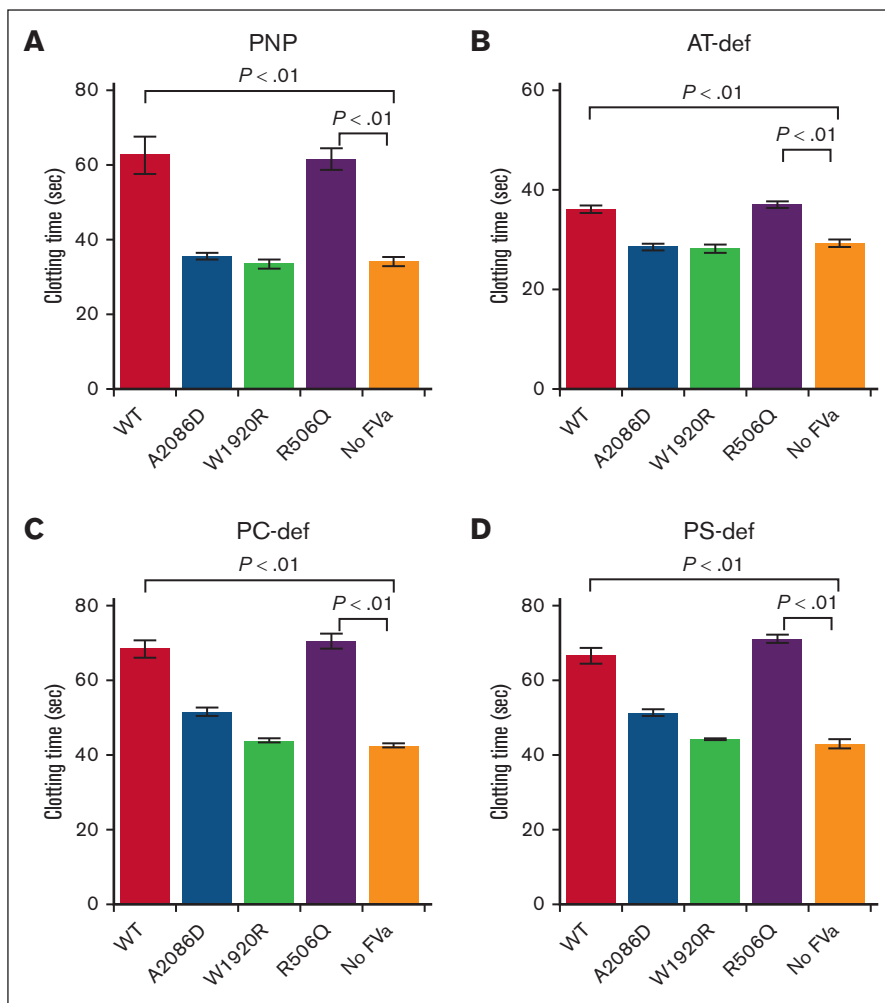


Figure 6. Inhibitory effects of the addition of FVa mutants to anticoagulant-deficient plasmas, determined with the diluted-PT reagent-based assay.

Diluted PT reagent was added to (A) pooled normal, (B) AT-deficient, (C) PC-deficient, and (D) PS-deficient plasma, and mixed with generated FVa mutant samples (f.c. 4.5 nM), followed by the addition of CaCl_2 . Clotting times were measured in seconds as described in "Methods."

Experiments were performed at least 3 times, and the average values \pm standard deviations are shown. One-way analysis of variance was performed on experimental data.

Acknowledgments

The authors thank Nanako Ohmichi and Hanako Shimo for excellent research support. SPR-based assay in this study was supported by the Center for Medical Research and Education, Graduate School of Medicine, Osaka University.

This research was supported by a research grant for Practical Research Project for Rare/Intractable Diseases, Japan Agency for Medical Research and Development (AMED) under grants 17ek0109210h0001 and 20ek0109481h0001.

Authorship

Contribution: N.S. performed all experiments, analyzed the data, interpreted the data, made the figures, and wrote the manuscript;

K.O. interpreted the data and edited the manuscript; J.Y. constructed the vector; K.H. constructed the vector and wrote the manuscript; Y.N., S.F., and M.T. analyzed and interpreted the data; and K.N. designed the experiments, interpreted the data, edited figures and manuscript, and supervised this study.

Conflict-of-interest disclosure: The authors declare no competing financial interests.

ORCID profiles: N.S., 0000-0002-0157-5215; K.O., 0000-0002-3046-6915; Y.N., 0000-0001-5422-2782; S.F., 0000-0002-4786-8945; M.T., 0000-0002-9348-9815.

Correspondence: Kenichi Ogiwara, Department of Pediatrics, Nara Medical University, 840 Shijo-cho, Kashihara, Nara 634-8522, Japan; email: ogiwarak@naramed-u.ac.jp.

References

- Dahlbäck B, Carlsson M, Svensson PJ. Familial thrombophilia due to a previously unrecognized mechanism characterized by poor anticoagulant response to activated protein C: prediction of a cofactor to activated protein C. *Proc Natl Acad Sci U S A*. 1993;90(3):1004-1008.
- Bertina RM, Koeleman BP, Koster T, et al. Mutation in blood coagulation factor V associated with resistance to activated protein C. *Nature*. 1994; 369(6475):64-67.

3. Rosing J, Tans G. Coagulation factor V: an old star shines again. *Thromb Haemost.* 1997;78(1):427-433.
4. Suzuki K, Dahlbäck B, Stenflo J. Thrombin-catalyzed activation of human coagulation factor V. *J Biol Chem.* 1982;257(11):6556-6564.
5. Foster WB, Nesheim ME, Mann KG. The factor Xa-catalyzed activation of factor V. *J Biol Chem.* 1983;258(22):13970-13977.
6. Walker FJ, Sexton PW, Esmon CT. The inhibition of blood coagulation by activated protein C through the selective inactivation of activated Factor V. *Biochim Biophys Acta.* 1979;571(2):333-342.
7. Suzuki K, Stenflo J, Dahlbäck B, Teodorsson B. Inactivation of human coagulation factor V by activated protein C. *J Biol Chem.* 1983;258(3):1914-1920.
8. Nicolaes GA, Tans G, Thomassen MC, et al. Peptide bond cleavages and loss of functional activity during inactivation of factor Va and factor VaR506Q by activated protein C. *J Biol Chem.* 1995;270(36):21158-21166.
9. Gale AJ, Xu X, Pellequer JL, Getzoff ED, Griffin JH. Interdomain engineered disulfide bond permitting elucidation of mechanisms of inactivation of coagulation factor Va by activated protein C. *Protein Sci.* 2002;11(9):2091-2101.
10. Gale AJ, Cramer TJ, Rozenshteyn D, Cruz JR. Detailed mechanisms of the inactivation of factor VIIIa by activated protein C in the presence of its cofactors, protein S and factor V. *J Biol Chem.* 2008;283(24):16355-16362.
11. O'Brien LM, Mastro M, Fay PJ. Regulation of factor VIIIa by human activated protein C and protein S: inactivation of cofactor in the intrinsic factor Xase. *Blood.* 2000;95(5):1714-1720.
12. Thorelli E, Kaufman RJ, Dahlbäck B. The C-terminal region of the factor V B-domain is crucial for the anticoagulant activity of factor V. *J Biol Chem.* 1998;273(26):16140-16145.
13. Lu D, Kalafatis M, Mann KG, Long GL. Comparison of activated protein C/protein S-mediated inactivation of human factor VIII and factor V. *Blood.* 1996;87(11):4708-4717.
14. Wood JP, Bunce MW, Maroney SA, Tracy PB, Camire RM, Mast AE. Tissue factor pathway inhibitor-alpha inhibits prothrombinase during the initiation of blood coagulation. *Proc Natl Acad Sci U S A.* 2013;110(44):17838-17843.
15. Petrillo T, Ayombil F, Van't Veer C, Camire RM. Regulation of factor V and factor V-short by TFPI α : relationship between B-domain proteolysis and binding. *J Biol Chem.* 2021;296:100234.
16. Dahlbäck B. Pro- and anticoagulant properties of factor V in pathogenesis of thrombosis and bleeding disorders. *Int J Lab Hematol.* 2016;38(suppl 1):4-11.
17. Dahlbäck B. Novel insights into the regulation of coagulation by factor V isoforms, tissue factor pathway inhibitor α , and protein S. *J Thromb Haemost.* 2017;15(7):1241-1250.
18. Al Dieri R, Bloemen S, Kelchtermans H, Wagenvoort R, Hemker HC. A new regulatory function of activated factor V: inhibition of the activation by tissue factor/factor VII(a) of factor X. *J Thromb Haemost.* 2013;11(3):503-511.
19. Williamson D, Brown K, Luddington R, Baglin C, Baglin T. Factor V Cambridge: a new mutation (Arg306 \rightarrow Thr) associated with resistance to activated protein C. *Blood.* 1998;91(4):1140-1144.
20. Chan WP, Lee CK, Kwong YL, Lam CK, Liang R. A novel mutation of Arg306 of factor V gene in Hong Kong Chinese. *Blood.* 1998;91(4):1135-1139.
21. Steen M, Norstrom EA, Tholander AL, et al. Functional characterization of factor V-Ile359Thr: a novel mutation associated with thrombosis. *Blood.* 2004;103(9):3381-3387.
22. Cai H, Hua B, Fan L, Wang Q, Wang S, Zhao Y. A novel mutation (g2172 \rightarrow c) in the factor V gene in a Chinese family with hereditary activated protein C resistance. *Thromb Res.* 2010;125(6):545-548.
23. Pezeshkpoor B, Castoldi E, Mahler A, et al. Identification and functional characterization of a novel F5 mutation (Ala512Val, FVB onn) associated with activated protein C resistance. *J Thromb Haemost.* 2016;14(7):1353-1363.
24. Nogami K, Shinozawa K, Ogiwara K, et al. Novel FV mutation (W1920R, FVNara) associated with serious deep vein thrombosis and more potent APC resistance relative to FVLeiden. *Blood.* 2014;123(15):2420-2428.
25. Gierula M, Salles-Crawley II, Santamaria S, et al. The roles of factor Va and protein S in formation of the activated protein C/protein S/factor Va inactivation complex. *J Thromb Haemost.* 2019;17(12):2056-2068.
26. Castoldi E, Hézard N, Mourey G, et al. Severe thrombophilia in a factor V-deficient patient homozygous for the Ala2086Asp mutation (FV Besançon). *J Thromb Haemost.* 2021;19(5):1186-1199.
27. Foster PA, Fulcher CA, Houghten RA, de Graaf Mahoney S, Zimmerman TS. Localization of the binding regions of a murine monoclonal anti-factor VIII antibody and a human anti-factor VIII alloantibody, both of which inhibit factor VIII procoagulant activity, to amino acid residues threonine351-serine365 of the factor VIII heavy chain. *J Clin Invest.* 1988;82(1):123-128.
28. Mimms LT, Zampighi G, Nozaki Y, Tanford C, Reynolds JA. Phospholipid vesicle formation and transmembrane protein incorporation using octyl glucoside. *Biochemistry.* 1981;20(4):833-840.
29. Soeda T, Nogami K, Nishiya K, et al. The factor VIIIa C2 domain (residues 2228-2240) interacts with the factor IXa Gla domain in the factor Xase complex. *J Biol Chem.* 2009;284(6):3379-3388.
30. Ding S, Wu X, Li G, Han M, Zhuang Y, Xu T. Efficient transposition of the piggyBac (PB) transposon in mammalian cells and mice. *Cell.* 2005;122(3):473-483.

31. Yusa K, Rad R, Takeda J, Bradley A. Generation of transgene-free induced pluripotent mouse stem cells by the piggyBac transposon. *Nat Methods*. 2009;6(5):363-369.
32. Niwa H, Yamamura K, Miyazaki J. Efficient selection for high-expression transfectants with a novel eukaryotic vector. *Gene*. 1991;108(2):193-199.
33. Okabe M, Ikawa M, Kominami K, Nakanishi T, Nishimune Y. 'Green mice' as a source of ubiquitous green cells. *FEBS Lett*. 1997;407(3):313-319.
34. Yusa K, Zhou L, Li MA, Bradley A, Craig NL. A hyperactive piggyBac transposase for mammalian applications. *Proc Natl Acad Sci U S A*. 2011;108(4):1531-1536.
35. Shen L, Dahlbäck B. Factor V and protein S as synergistic cofactors to activated protein C in degradation of factor VIIIa. *J Biol Chem*. 1994;269(29):18735-18738.
36. Norström E, Thorelli E, Dahlbäck B. Functional characterization of recombinant FV Hong Kong and FV Cambridge. *Blood*. 2002;100(2):524-530.
37. Hemker HC, Giesen P, Al Dieri R, et al. Calibrated automated thrombin generation measurement in clotting plasma. *Pathophysiol Haemost Thromb*. 2003;33(1):4-15.
38. Eaton D, Rodriguez H, Vehar GA. Proteolytic processing of human factor VIII. Correlation of specific cleavages by thrombin, factor Xa, and activated protein C with activation and inactivation of factor VIII coagulant activity. *Biochemistry*. 1986;25(2):505-512.
39. Nogami K, Wakabayashi H, Fay PJ. Mechanisms of factor Xa-catalyzed cleavage of the factor VIIIa A1 subunit resulting in cofactor inactivation. *J Biol Chem*. 2003;278(19):16502-16509.
40. Li MA, Turner DJ, Ning Z, et al. Mobilization of giant piggyBac transposons in the mouse genome. *Nucleic Acids Res*. 2011;39(22):e148.
41. Matsui H, Fujimoto N, Sasakawa N, et al. Delivery of full-length factor VIII using a piggyBac transposon vector to correct a mouse model of hemophilia A. *PLoS One*. 2014;9(8):e104957.
42. Petrillo T, Small JC, Camire RM. Addition of histone deacetylase inhibitors increases recombinant factor V expression in BHK cells, [abstract]. *Res Pract Thromb Haemost*. 2020;4(suppl 1). Abstract PB0227.
43. Krishnaswamy S, Williams EB, Mann KG. The binding of activated protein C to factors V and Va. *J Biol Chem*. 1986;261(21):9684-9693.
44. Yegneswaran S, Kojima Y, Nguyen PM, Gale AJ, Heeb MJ, Griffin JH. Factor Va residues 311-325 represent an activated protein C binding region. *J Biol Chem*. 2007;282(39):28353-28361.
45. Ruben EA, Rau MJ, Fitzpatrick JAJ, Di Cera E. Cryo-EM structures of human coagulation factors V and Va. *Blood*. 2021;137(22):3137-3144.
46. Zöller B, Svensson PJ, He X, Dahlbäck B. Identification of the same factor V gene mutation in 47 out of 50 thrombosis-prone families with inherited resistance to activated protein C. *J Clin Invest*. 1994;94(6):2521-2524.
47. Vincent LM, Tran S, Livaja R, Bensed TA, Milewicz DM, Dahlbäck B. Coagulation factor V (A2440G) causes east Texas bleeding disorder via TFPI α . *J Clin Invest*. 2013;123(9):3777-3787.
48. Santamaria S, Reglińska-Matveyev N, Gierula M, et al. Factor V has an anticoagulant cofactor activity that targets the early phase of coagulation. *J Biol Chem*. 2017;292(22):9335-9344.
49. van Doorn P, Rosing J, Duckers C, Hackeng TM, Simioni P, Castoldi E. Factor V has anticoagulant activity in plasma in the presence of TFPI α : difference between FV1 and FV2. *Thromb Haemost*. 2018;118(7):1194-1202.